

Received: 2015.09.08
Accepted: 2015.10.12
Published: 2016.03.02

Evaluation of Hepatic Tumors Using Intravoxel Incoherent Motion Diffusion-Weighted MRI

Authors' Contribution:
Study Design A
Data Collection B
Statistical Analysis C
Data Interpretation D
Manuscript Preparation E
Literature Search F
Funds Collection G

AE **Mingjie Wang***
BF **Xudan Li***
AD **Jianxun Zou**
BF **Xugao Chen**
D **Shuyan Chen**
B **Wanqing Xiang**

Department of Radiology, Lishui People's Hospital, Lishui, Zhejiang, P.R. China

* Mingjie Wang and Xudan Li contributed equally to the work and thus share the first authorship

Corresponding Author: Jianxun Zou, e-mail: lsrmywmj@163.com

Source of support: Departmental sources

Background: This study aimed to evaluate the diagnostic value of the D value, D* value, and f magnitude for identifying benign and malignant hepatic tumors using intravoxel incoherent motion (IVIM) diffusion-weighted imaging (DWI).





Material/Methods: Data of 89 cases (123 lesions) with hepatic tumor confirmed by surgical pathology and postoperative follow-up were retrospectively collected. Among these cases, 40 cases were benign hepatic tumors (57 lesions) and 49 cases were malignant hepatic tumors (66 lesions). All subjects underwent conventional MRI with T₁WI, T₂WI, multi-b-value DWI, and dynamic enhanced LAVA scan. Diffusion-weighted images with 11 b values (0, 10, 20, 30, 50, 80, 100, 200, 400, 800, and 1000 s/mm²) were obtained to calculate true molecular diffusion (D), perfusion-related diffusion coefficient (D*), and perfusion fraction (f). The diagnostic performance in differentiating between malignant and benign hepatic lesions was analyzed.

Results: Malignant lesions had a significantly lower D value ($[1.04 \pm 0.34] \times 10^{-3}$ mm²/s) and D* value ($[16.5 \pm 7.7] \times 10^{-3}$ mm²/s) compared to benign lesions (D value: $[1.70 \pm 0.55] \times 10^{-3}$ mm²/s, $P < 0.01$; D* value: $[21.7 \pm 9.9] \times 10^{-3}$ mm²/s, $P < 0.01$). There was no statistically significant difference in f values between malignant (23.3 ± 9.5) and benign lesions (33.5 ± 14.9, $P = 0.13$). In addition, D exhibited a better diagnostic performance than D* in terms of the area under the curve, sensitivity, and specificity when identifying malignancies from benign lesions.

Conclusions: D and D* are significant parameters for diagnosing hepatic tumors. Moreover, the D value is a more reliable parameter in distinguishing benign and malignant hepatic tumors.

MeSH Keywords: **Diffusion Magnetic Resonance Imaging • Liver Diseases • Liver Neoplasms**

Full-text PDF: <http://www.medscimonit.com/abstract/index/idArt/895909>

 2623  4  3  27



Background

With the rapid development of magnetic resonance imaging (MRI) technology such as improved MRI gradient performance, multichannel surface receiver coils, and parallel imaging techniques, functional MRI technology has brought revolutionary progress in the diagnosis and study of diseases [1]. Diffusion-weight imaging (DWI) can reflect the pathological and physiological information of the lesion on the basis of the microscopic mobility of water, which is called the Brownian movement in organisms with various diseases, and it also has an important role in the identification of hepatic tumors [2–9]. Previous studies have suggested that the apparent diffusion coefficient (ADC) of hepatic tumor lesions has distinct differences between benign and malignant tumors, which can distinguish the property of a tumor [10,11]. However, inherent limitations exist in diagnosis based on a single exponential model, especially losing sight of the effect of the arteriole-capillary-venule microcirculation in living tissues on ADC values [12]. In 1986, Le Bihan et al. proposed the principles of intravoxel incoherent motion (IVIM) [10] and suggested that using a more sophisticated approach to describe the relationship between signal attenuation in tissues with increasing b value would enable quantitative parameters that separately reflect tissue diffusivity and tissue microcapillary perfusion to be estimated. In 1988, Le Bihan et al. used a phantom that could show the effects of perfusion using DW imaging [13]. Yamada et al. initially applied IVIM to the abdomen in 1999 to evaluate the diffusion coefficient of lesions in the abdominal viscera [14].

IVIM can provide quantitative parameters for the movement of water molecules in tissues and reflect the perfusion condition of the tissue [15]. In fact, IVIM separates ‘diffusion’ and ‘perfusion’ through a special diffusion-weighted imaging sequence at the voxel level [15]. IVIM-DWI can be obtained through multiple b values, and emphasizes the combined application of the low b value ($<200 \text{ s/mm}^2$) and high b value ($>200 \text{ s/mm}^2$) to accurately and effectively detect and measure the ADC value of lesions [16]. The IVIM-DWI technique can be used to estimate the diffusion coefficient of slow or nonperfusion-related diffusion-based molecular diffusion (D), the diffusion coefficient of fast or perfusion-related diffusion based diffusion (D^*), and the perfusion-related diffusion fraction (f) in the voxel. D reflects tissue diffusivity and D^* reflects microcapillary perfusion [17].

This research used the double exponential model to estimate the D value, D^* value and f magnitude and compare the diagnostic performance of these parameters in hepatic tumors.

Material and Methods

Patients

This study was approved by the local ethics committee and written informed consent was obtained from each subject before the examination. From January 2014 to October 2014, a total of 103 subjects with suspicious hepatic tumors underwent multiple-b-value IVIM-DWI. A total of 123 focal hepatic lesions in 89 patients were included in this study after surgical pathological confirmation. Among the 89 patients, 52 patients were male and 37 patients were female. Mean age was 69.7 years old with an age range of 39 to 85 years old. Patients with definite diagnosis were divided into 2 groups according to the extent of tumor progress: benign tumor group (40 cases, 57 lesions) and malignant tumor group (49 cases, 66 lesions). Final diagnoses were as follows: hemangioma (47 lesions in 31 cases), liver abscess (5 lesions in 4 cases), focal nodular hyperplasia (4 lesions in 4 cases), liver hamartoma (1 lesion in 1 case), hepatocellular carcinoma (40 lesions in 30 cases), metastatic liver tumor (20 lesions in 13 cases), and cholangiocarcinoma (6 lesions in 6 cases, Table 1). Primary tumors of the metastatic liver tumor were as follows: colorectal carcinoma (7 cases), pancreatic carcinoma (2 cases), gastric carcinoma (2 cases), breast cancer (1 case), and ampullary carcinoma (1 case). Size (given as mean \pm standard deviation and range) of the hepatic carcinoma, cholangiocarcinoma, metastatic liver tumor, hepatocellular carcinoma, focal nodular hyperplasia, abscess and hamartoma were $3.11\pm 1.92 \text{ cm}$ (1.68–4.50 cm), $3.12\pm 1.03 \text{ cm}$ (1.95–6.43 cm), $1.72\pm 1.35 \text{ cm}$ (1.30–3.90 cm), $2.84\pm 1.79 \text{ cm}$ (1.50–7.50 cm), $3.17\pm 1.74 \text{ cm}$ (1.70–6.00 cm), $2.62\pm 1.43 \text{ cm}$ (1.60–5.00 cm), and 4.41 cm, respectively.

Inclusion criteria were as follows: (1) patients with focal liver lesions detected by computed tomography (CT) or ultrasound examination, (2) patients who were not contraindicated to the MR examination, (3) patients with focal hepatic lesion $>2 \text{ cm}$ in diameter, and (4) conclusive diagnosis of the lesion using either pathological or aspiration biopsy confirmation.

Exclusion criteria were as follows: (1) patients who were treated by transarterial chemoembolization or radiofrequency ablation, (2) patients whose images were of unacceptable quality for the evaluation of focal hepatic lesions on DWI, (3) patients who are unable to tolerate the examination, and (4) patients who did not achieve a definite diagnosis.

MRI

MRI was performed using a 3.0T whole-body scanner (Discovery MR750, GE Healthcare Systems; Milwaukee, WI, USA) with a GE 8-channel phased-array coil. All subjects were subjected to

Table 1. Baseline characteristics of benign and malignant hepatic lesions.

	Benign tumors	Malignant tumors
Number of patients	40	49
Age (years)	43.1±6.97	51.2±10.6
Gender ratio (Male: Female)	23: 24	29: 13
Lesions	57	66
	Hemangioma (n=47)	Hepatocellular carcinoma (n=40)
	Hepatapostema (n=5)	Metastatic liver tumor (n=20)
	FNH (n=4)	Cholangiocarcinoma (n=6)
	Hamartoma (n=1)	

FNH – focal nodular hyperplasia.

limosis for 4–8 h before the examination and respiratory training to achieve consistency of breathing extent and frequency.

Routine MRI protocols consisted of transverse T1-weighted imaging (T1WI) using 3D gradient-echo pulse LAVA (liver acquisition with volume acceleration) sequences, transverse breath-trigger fat suppressed fast recovery fast spin-echo (FRFSE) T2-weighted imaging (T2WI), and coronal breath-trigger fat suppressed FRFSE T2WI. IVIM-DWI with respiratory triggering was performed with the following scanning parameters: TE=79 ms, TR=6000 ms, matrix size=128×160, FOV from 36×36 cm to 40×40 cm, slice thickness=7 mm, gap=1 mm and scanning time=256 s. Eleven b-values were used: 0, 10, 20, 30, 50, 80, 100, 200, 400, 800, and 1000 s/mm². For b values in ranges of 0–30 s/mm², 50–200 s/mm² and 400–1000 s/mm², NEX was 3, 2, and 6, respectively.

Transverse and coronal contrast-enhanced DWI imaging was performed with a 3D T1-weighted gradient-echo pulse LAVA sequence after the administration of gadopentetate dimeglumine (GD-DTPA; Beilu Pharmaceutical, Beijing, China) into the elbow vein at a dose of 0.1 mmol/kg with a rate of 2.5–3 ml/s by high-pressure syringe. The contrast agent was followed by using an intravenous bolus administration of 20 ml of saline at the same rate. Scanning parameters were as follows: matrix size=288×192, slice thickness=2–5 mm, and the layer number of scanning ranged from 70 to 100. TR=3.7 ms, TE=1.7 ms, rotation angle=12° and breath holding time=12–17 s. The arterial, portal venous and delayed phase scans were performed 18–20 s, 55–60 s and 3 min after contrast injection, respectively.

Image analysis

Three diffusivity parameters were defined as follows: diffusion coefficient of slow or nonperfusion-related diffusion-based molecular diffusion (D, 10⁻³ mm²/s) represents true molecular diffusion, diffusion coefficient of fast or perfusion-related diffusion based diffusion (D*, 10⁻³ mm²/s) represents perfusion-related diffusion, and perfusion-related diffusion fraction (f, %)

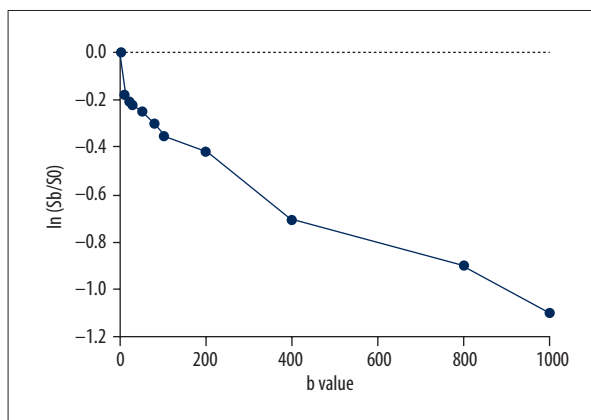


Figure 1. Plot shows ln(Sb/S0) of relative signal intensity vs. b values from primary hepatocellular carcinoma. The signal attenuation curve shows a hockey-stick appearance at low b-values, which is indicative of a perfusion effect.

represents fractional volume occupied in the voxel by flowing spins. These diffusivity values were calculated using the IVIM model equation described by Le Bihan et al. [10]:

$$Sb/S0 = (1-f) \times \exp(-bD) + f \times \exp(-b[D+D^*])$$

Sb is the signal intensity for a given b value and S0 is the signal intensity at b=0 s/mm². D was initially determined by the linear least square approach using DWI with a b-value >200 s/mm². D* and f were calculated by the nonlinear least-squares approach using the Nelder-Mead method. Figure 1 plots ln(Sb/S0) of relative signal intensity vs. b values from cases of primary hepatocellular carcinoma.

All acquired images were analyzed on a GE Advantage Workstation 4.6 using the local software of the machine Functool (GE Healthcare, Milwaukee, WI, USA) [18] prior to surgery and before pathologic results were known. Two clinically experienced radiologists with more than five 5 years of experience in interpreting hepatic MR images, who were blinded to the final

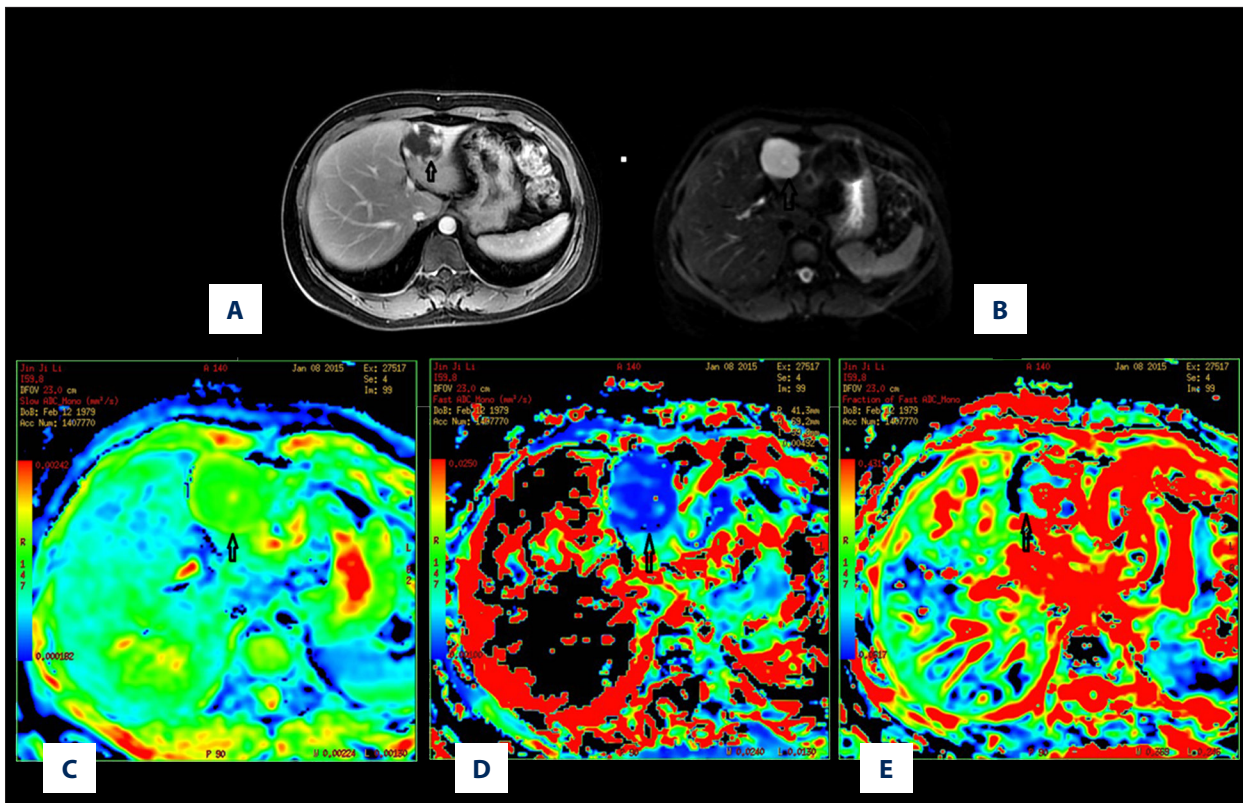


Figure 2. A 45-year-old female patient with hepatic cavernous hemangioma. (A) Contrast-enhanced DWI during the delayed phase showing a multi-nodular enhancement on the edge of the lesion located in segment III of the liver. (B) Mapping of the signal intensity of the lesion is much higher than hepatic parenchyma when $b=0$ s/mm². (C) Mapping of the estimated value of the D parameter. The average value in the lesion ROI was $D=2.27 \times 10^{-3}$ mm²/s. (D) Mapping of the estimated value of the D* parameter. The average value in the lesion ROI was $D^*=15.3 \times 10^{-3}$ mm²/s. (E) Mapping of the perfusion-related diffusion fraction (f) with a value of 33.3%.

Table 2. Comparison of IVIM Parameters between malignant and benign hepatic lesions (means \pm SD).

	Benign tumors	Malignant tumors	P value
D (10 ⁻³ mm ² /s)	1.70 \pm 0.55	1.04 \pm 0.23	<0.01
D* (10 ⁻³ mm ² /s)	21.7 \pm 9.9	16.5 \pm 7.7	<0.01
f (%)	33.5 \pm 14.9	23.3 \pm 9.5	0.13

D – true molecular diffusion; D* – perfusion-related diffusion coefficient; f – perfusion fraction.

histology or biopsy, evaluated each of the MR images independently. Decisions were obtained by consensus. Routine T1WI, T2WI, and dynamic enhanced LAVA T1WI were provided to confirm the location and size of the lesion when IVIM-DWI images were evaluated (Figure 2A and Figure 3A, 3B). ROIs were placed on an image with $b=0$ (Figure 2B and Figure 3C). The software automatically copied the ROI to each image ($b=10$ –1,000 s/mm²) and calculated the average of the signals within the ROI for each image while simultaneously recording the D value, D* value and f value, respectively (Figure 2C–2E and Figure 3D–3F). In focal hepatic lesions, ROIs were placed in order to avoid necrosis or hemorrhage, and ROIs were drawn as large as possible to cover the solid part of the lesions. Mean ROI area was 22.4–29.3 mm².

Statistical analysis

Data were analyzed using commercial software (IBM SPSS v.19, Armonk, NY; MedCalc v.12, Mariakerke, Belgium). Data were expressed as means \pm standard deviation (SD). Shapiro-Wilk test was used to examine the normality. Diffusion parameters of benign and malignant tumors were compared by Mann-Whitney U test. Diffusion parameter results between malignant tumor types were compared by Kruskal-Wallis test followed by Bonferroni-corrected Mann-Whitney U test. Receiver operating characteristic (ROC) analysis was performed for lesion discriminability between malignant and benign hepatic lesions. A P value <0.05 was considered statistically different.

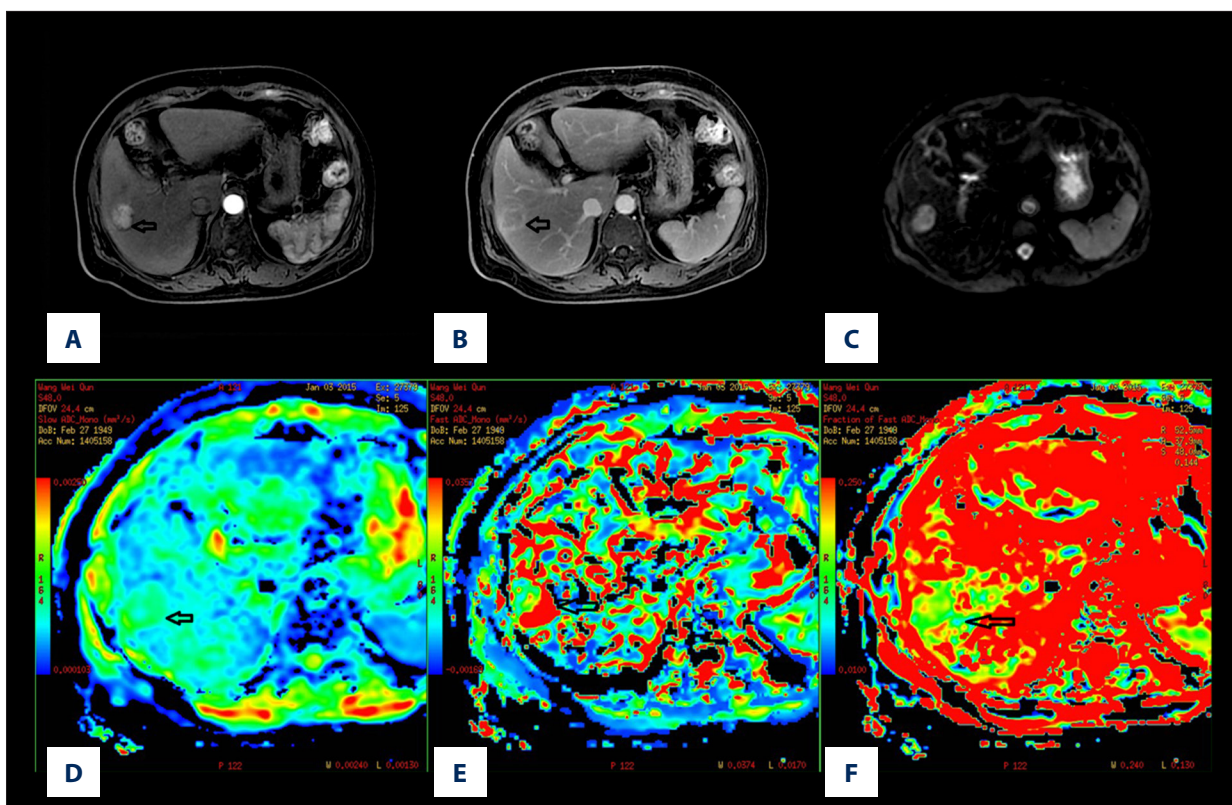


Figure 3. A 63-year-old male man with primary hepatocellular carcinoma. (A) Contrast-enhanced DWI during the arterial phase showing lesion enhancement in segment IV of the liver. (B) The lesion enhancement degree in the delayed phase decreases obviously compared to that of the arterial phase. (C) The signal of the lesion is slightly higher than hepatic parenchyma when $b=0$ s/mm². (D) Mapping of the estimated value of the D parameter. The average value in the lesion ROI was $D=1.19 \times 10^{-3}$ mm²/s. The signal of the lesion is slightly lower than hepatic parenchyma. (E) Mapping of the estimated value of the D* parameter. The average value in the lesion ROI was $D^*=22.4 \times 10^{-3}$ mm²/s. The signal of the lesion is slightly lower than hepatic parenchyma. (F) Mapping of the perfusion-related diffusion fraction (f) with a value of 12.2%.

Table 3. Diffusion parameters for all malignant tumor types among groups.

	D (10 ⁻³ mm ² /s)	D* (10 ⁻³ mm ² /s)	f (%)
Hepatocellular carcinoma	0.98±0.28*	21.17±8.34#	26.43±7.24
Cholangiocarcinoma	1.19±0.35	15.68±4.11#	16.98±9.9
Metastatic liver tumor	0.93±0.36*	12.22±3.71	21.98±8.54
P values			
Hepatocellular carcinoma vs. cholangiocarcinoma	0.002	0.312	0.342
Hepatocellular carcinoma vs. metastatic liver tumor	0.409	0.001	0.987
Cholangiocarcinoma vs. metastatic liver tumor	0.021	0.016	0.634

* $P < 0.05$ vs. cholangiocarcinoma; # $P < 0.05$ vs. metastatic liver tumor; D – true molecular diffusion; D* – perfusion-related diffusion coefficient; f – perfusion fraction.

Results

Both the D value ($[1.04 \pm 0.34] \times 10^{-3}$ mm²/s) and D* value ($[16.5 \pm 7.7] \times 10^{-3}$ mm²/s) in malignant lesions were significantly lower than in benign lesions (D value $[1.70 \pm 0.55] \times 10^{-3}$ mm²/s, $P < 0.01$; D* value $[21.7 \pm 9.9] \times 10^{-3}$ mm²/s, $P < 0.01$). There was no

statistically significant difference in f value between malignant (23.3 ± 9.5) and benign (33.5 ± 14.9) lesions ($P = 0.13$, Table 2).

Results of diffusion and perfusion-related parameters by tumor type are shown in Table 3. Cholangiocarcinoma presented significantly higher D values than metastatic liver tumor ($P = 0.021$)

Table 4. Diagnostic performance for distinguishing between malignant and benign hepatic lesions.

	D	D*	P value
AUC (95% CI)	0.98 (0.94–1.00)	0.884 (0.81–0.91)	<0.05
Cut-off values (10^{-3} mm ² /s)	1.295	21.85	
Sensitivity	96.2%	90.6%	
Specificity	91.4%	82.9%	

AUC – area under the curve; D – true molecular diffusion; D* – perfusion-related diffusion coefficient.

and hepatocellular carcinoma ($P=0.002$). Similarly, metastatic liver tumor had significantly lower D* values than cholangiocarcinoma ($P=0.016$) and hepatocellular carcinoma ($P=0.001$).

According to ROC analysis, the average area under the ROC curve for predicting malignant lesions was 0.88 (0.81–0.91) for D* value and 0.98 (0.94–1.00) for D value ($P<0.05$, Table 4). Optimal cutoff values calculated by ROC analysis (D, 1.295×10^{-3} mm²/s and D*, 21.85×10^{-3} mm²/s) provided sufficiently high sensitivity and specificity for both D (96.2% and 91.4%, respectively) and D* (90.6% and 82.9%, respectively) values (Table 4).

Discussion

Functional MR images can reflect the random motion (Brownian movement) of water molecules in living tissue. However, quantitative ADC values can also be affected by physiological activity and the perfusion effect of the capillary network [19]. The double exponential model with multi-b-values separates the diffusion and perfusion (microcirculation) of water molecules. It more closely approximates the real ADC of the biological tissue, which reflects DWI better than the single exponential model [20].

The IVIM double exponential model assumes that tissue diffusion consists of 2 parts: Brownian movement (D) due to molecular diffusion, and fast perfusion movement (D*) due to blood flow in smaller vessels. D is the static tissue molecular diffusion (true diffusion coefficient), which is calculated by selecting the high b value (>200 /mm²) and eliminating the perfusion component. D* denotes the perfusion-diffusion coefficient, which is the perfusion-related diffusion coefficient due to blood circulation. Perfusion composition of tissue microcirculation is sensitive to MR signal attenuation with low b values (<200 /mm²) [21]. The perfusion fraction f represents the fractional volume occupied in the voxel by flowing spins linked to the intravascular component or to the microcirculation. D* is closely associated with blood vessel density in tumor tissues, and f value increases with the growth of the tissue perfusion component [22]. In this study, D* values were

much greater than the corresponding D values, which indicate that D* is sensitive to MR signal attenuation when b value is low. The D, D*, and f values in our study are similar to a previous study in hepatic adenoma, hepatic cavernous hemangioma, hepatocellular carcinoma, metastatic liver tumor, and cholangiocarcinoma patients [23]. However, the study of Ichikawa et al. [17] reported higher D, D*, and f values than those in our study. These may be due to the difference on the manual ROI drawing (manual ROI method) and the number of patients or lesions. The attribute of the hypovascularity of metastatic liver tumors in this study may also affect these outcomes.

In this study, we found both D and D* values in malignant lesions were significantly lower than in benign lesions, which is consistent with the findings of Ichikawa et al. [17]. This may be due to the similar distribution of the samples. In contrast to our findings, the study of Doblaz et al. [24] reported that pure diffusion coefficients (D) were significantly lower in malignant tumors than in benign tumors, while perfusion-related diffusion parameters (D*) did not significantly differ between these 2 groups, which was due to the large number of benign hepatocellular lesions (FNH and adenomas) in their study.

The D* value of metastatic liver tumors is lower than hepatocellular carcinoma and cholangiocarcinoma, which may be due to the hypovascular property of the metastatic liver tumor. Our findings are consistent with those of a previous study, which reported that D* and f values can reflect the condition of the blood supply, and these values are higher in hypervascular hepatic tumors than in hypovascular hepatic tumors [9].

This study also used the ROC curve to evaluate the diagnostic efficiency of D, D*, and f. The ROC curve presents the optimal threshold of D for the diagnosis of benign and malignant tumors is 1.295×10^{-3} mm²/s. Sensitivity (91.4%) and specificity (96.2%) of the D value are both relatively high for identifying the maximum AUC (0.976), indicating the highest diagnostic efficiency of the D value. These may be caused by the following. (1) The most obvious difference between benign and malignant tumors is the component of abnormal cell proliferation. Altered nucleo-cytoplasmic ratio and nuclear atypia in malignant tumor cell induce the limited diffusion of water

molecules and increase the true diffusion of the tissue. (2) The component separation of perfusion-diffusion and true molecular diffusion by the double exponential model resulted in the calculation, in which the D value is closer to the actual ADC of the biological tissue. The perfusion-diffusion is due to the irregular perfusion of the microcirculation in the blood capillary. The relatively small sample size and the selection of lesion types in this study may have affected interpretation of results. Therefore, further studies are warranted.

More realistic D, D*, and f values can be obtained by using more DWI images of low b values and high b values during IVIM imaging, contributing to the qualitative and quantitative identification of the diagnosis. D and D* are both valuable in the diagnosis of hepatic tumors, but D is more reliable in property identification. The diagnostic value of the perfusion parameter obtained by IVIM may reduce the dependency for liver contrast medium clinically. IVIM is an ideal examination method when dynamic enhanced scan period (arterial phase) fails or for contrast medium sensitivity, especially for senile patients and infants.

This study has several limitations. First, this is a retrospective study. Thus, there is an overbalance in the distribution of tumor types, which is limited by the subjects in the hospital. Second, using 3 parameters is unstable, in contrast to using a single parameter; which can easily cause errors in the D* value. In particular, when the f value is small (low perfusion proportion), the quality of the D* image decreases and the chance for more errors on the D* value is higher [25]. Third, the liver is a locomotive organ that can affect IVIM parameters [26,27]. Finally, multi-b-value technology prolongs scanning time, which is onerous for patients.

Conclusions

IVIM DWI can provide more essential D, D*, and f values by using sufficiently low b values and high b values, which contributes to the qualitative and quantitative diagnosis of hepatic tumors. The D value was proven to be a more reliable parameter than the D* value for distinguishing between malignant and benign hepatic lesions.

Conflict of interest

The authors declare that they have no conflict of interest.

References:

- Koh DM, Collins DJ: Diffusion-weighted MRI in the body: applications and challenges in oncology. *Am J Roentgenol*, 2007; 188: 1622–35
- Parikh T, Drew SJ, Lee VS et al: Focal liver lesion detection and characterization with diffusion-weighted MR imaging: comparison with standard breath-hold T2-weighted imaging. *Radiology*, 2008; 246: 812–22
- Taouli B, Ehman RL, Reeder SB: Advanced MRI methods for assessment of chronic liver disease. *Am J Roentgenol*, 2009; 193: 14–27
- Yang DM, Jahng GH, Kim HC et al: The detection and discrimination of malignant and benign focal hepatic lesions: T2 weighted vs. diffusion-weighted MRI. *Br J Radiol*, 2011; 84: 319–26
- Coenegrachts K, Delanote J, Ter Beek L et al: Improved focal liver lesion detection: comparison of single-shot diffusion-weighted echoplanar and single-shot T2 weighted turbo spin echo techniques. *Br J Radiol*, 2007; 80: 524–31
- Lewis S, Kamath A, Chatterji M et al: Diffusion-weighted imaging of the liver in patients with chronic liver disease: comparison of monopolar and bipolar diffusion gradients for image quality and lesion detection. *Am J Roentgenol*, 2015; 204: 59–68
- Bouchaibi SE, Coenegrachts K, Bali MA et al: Focal liver lesions detection: Comparison of respiratory-triggering, triggering and tracking navigator and tracking-only navigator in diffusion-weighted imaging. *Eur J Radiol*, 2015; 84(10): 1857–65
- Furuta A, Isoda H, Yamashita R et al: Comparison of monopolar and bipolar diffusion weighted imaging sequences for detection of small hepatic metastases. *Eur J Radiol*, 2014; 83: 1626–30
- Yoon JH, Lee JM, Yu MH et al: Evaluation of hepatic focal lesions using diffusion-weighted MR imaging: comparison of apparent diffusion coefficient and intravoxel incoherent motion-derived parameters. *J Magn Reson Imaging*, 2014; 39: 276–85
- Le Bihan D, Breton E, Lallemand D et al: MR imaging of intravoxel incoherent motions: application to diffusion and perfusion in neurologic disorders. *Radiology*, 1986; 161: 401–7
- Patel J, Sigmund EE, Rusinek H et al: Diagnosis of cirrhosis with intravoxel incoherent motion diffusion MRI and dynamic contrast-enhanced MRI alone and in combination: preliminary experience. *J Magn Reson Imaging*, 2010; 31: 589–600
- Goshima S, Kanematsu M, Kondo H et al: Diffusion-weighted imaging of the liver: optimizing b value for the detection and characterization of benign and malignant hepatic lesions. *J Magn Reson Imaging*, 2008; 28: 691–97
- Le Bihan D, Breton E, Lallemand D et al: Separation of diffusion and perfusion in intravoxel incoherent motion MR imaging. *Radiology*, 1988; 168: 497–505
- Yamada I, Aung W, Himeno Y et al: Diffusion coefficients in abdominal organs and hepatic lesions: evaluation with intravoxel incoherent motion echo-planar MR imaging. *Radiology*, 1999; 210: 617–23
- Koh DM, Collins DJ, Orton MR: Intravoxel incoherent motion in body diffusion-weighted MRI: reality and challenges. *Am J Roentgenol*, 2011; 196: 1351–61
- Li YH, Lu JP, Duan XJ: A preliminary study of pediatric brain tumors using multi-component diffusion weighted imaging. *Radio Pract*, 2012; 2: 018
- Ichikawa S, Motosugi U, Ichikawa T et al: Intravoxel incoherent motion imaging of focal hepatic lesions. *J Magn Reson Imaging*, 2013; 37: 1371–76
- Wagih A, Mohsen L, Rayan MM et al: Posterior reversible encephalopathy syndrome (PRES): Restricted diffusion does not necessarily mean irreversibility. *Pol J Radiol*, 2015; 80: 210–16
- Le Bihan D, Turner R, Moonen CT, Pekar J: Imaging of diffusion and microcirculation with gradient sensitization: design, strategy, and significance. *J Magn Reson Imaging*, 1991; 1: 7–28
- Nilsen LB, Fangberget A, Geier O, Seierstad T: Quantitative analysis of diffusion-weighted magnetic resonance imaging in malignant breast lesions using different b value combinations. *Eur Radiol*, 2013; 23: 1027–33
- Dyvorne HA, Galea N, Nevers T et al: Diffusion-weighted imaging of the liver with multiple b values: effect of diffusion gradient polarity and breathing acquisition on image quality and intravoxel incoherent motion parameters – a pilot study. *Radiology*, 2013; 266: 920–29

22. Lewin M, Fartoux L, Vignaud A et al: The diffusion-weighted imaging perfusion fraction f is a potential marker of sorafenib treatment in advanced hepatocellular carcinoma: a pilot study. *Eur Radiol*, 2011; 21: 281–90
23. Lu GG, Gao XM, Cheng JL et al: Evaluation of intravoxel incoherent motion diffusion-weighted imaging in differentiating benign from malignant hepatic neoplasm. *J Clin Radio*, 2014; 33: 1013–17
24. Doblas S, Wagner M, Leitao HS et al: Determination of malignancy and characterization of hepatic tumor type with diffusion-weighted magnetic resonance imaging: comparison of apparent diffusion coefficient and intravoxel incoherent motion-derived measurements. *Invest Radiol*, 2013; 48: 722–28
25. King MD, van Bruggen N, Busza AL et al: Perfusion and diffusion MR imaging. *Magn Reson Med*, 1992; 24: 288–301
26. Andreou A, Koh DM, Collins DJ et al: Measurement reproducibility of perfusion fraction and pseudodiffusion coefficient derived by intravoxel incoherent motion diffusion-weighted MR imaging in normal liver and metastases. *Eur Radiol*, 2013; 23: 428–34
27. Sigmund EE, Vivier PH, Sui D et al: Intravoxel incoherent motion and diffusion-tensor imaging in renal tissue under hydration and furosemide flow challenges. *Radiology*, 2012; 263: 758–69